

# Optimal Doping Density for Quantum-Well Infrared Photodetector Performance

Y. Yang, H. C. Liu, *Fellow, IEEE*, W. Z. Shen, N. Li, W. Lu, Z. R. Wasilewski, and M. Buchanan

**Abstract**—We present a systematic study on a set of *n*-type GaAs–AlGaAs quantum-well infrared photodetectors (QWIPs) with varying Si doping density in the wells. It is revealed that the increase in doping density enhances proportionally the absorption efficiency and responsivity while increasing exponentially the dark current and hence the dark current noise. We experimentally confirm the theoretically predicted optimum conditions for background-limited infrared performance temperature and detector-noise-limited detectivity. It is suggested that, to achieve the optimal QWIP performance, the doping density in the wells should be determined according to application and the desired operating temperature. We point out that a simulation is highly recommended to achieve the best possible performance since the choice of doping may not be obvious. As shown here, an optimized doping for temperature is actually the worst for detectivity for the particular set of samples.

**Index Terms**—Background-limited infrared performance (BLIP) temperature, detectivity, doping density, optimal condition, quantum-well infrared photodetectors (QWIPs).

## I. INTRODUCTION

THE quantum-well infrared photodetector (QWIP) [1]–[3] is by now an established technology. Large focal-plane arrays are being used in space applications [4] and are being implemented into military vehicles [5]. High-speed QWIPs [6] are being employed in various laboratories, enabling cutting-edge science exploration [7]. By now, for a standard QWIP structure, guidelines for all device parameters for optimal detector performance have been established [2]. Systematic experimental verifications to achieve the optimal performance have been carried

out on most of the device parameters [8]–[11] except for the doping density in the well. Gunapala *et al.* [12] investigated the effect of doping on the QWIP performance; however, the QW design used there was an extremely bound-to-continuum one, and no clear optimum was found for blackbody detectivity as a function of doping. A standard QWIP is simply a doped multiple quantum well (MQW) structure between two contact layers. The most commonly used material system is GaAs–AlGaAs with *n*-type doping usually with Si. The doping is commonly placed in the wells and the barrier is usually wide to suppress dark current. For the optimal design, once a desired detection wavelength is specified, the well width and barrier height (determined by [Al] fraction) are fixed based on having the upper state in resonance with the barrier top [10]. This QW optimal configuration has been tested and verified experimentally [8]. The number of QWs should be large enough to give a sufficient absorption [2], [9]. The barrier width should be larger than a critical value given a background for the application [2], [11].

In this paper, we present a comprehensive study of the effect of doping density on the QWIP performance. We characterize a systematic set of QWIP samples with otherwise identical device parameters but the doping density. We measure the device key performance characteristics and compare them with the standard theory of QWIPs. The merit of this work relates to the clear and unambiguous experimental verification of the theoretically predicted optimal conditions. This puts confidence into the predictive power of the standard QWIP theory. The work further gives guidelines in choosing the doping density and points out situations to avoid.

## II. EXPERIMENTAL DETAILS

The QWIPs studied here are fabricated by molecular beam epitaxy (MBE) on semi-insulating GaAs substrates. The MQW structure that is composed of 100 repeats of GaAs (54 Å thick)/Al<sub>0.24</sub>Ga<sub>0.76</sub>As (300 Å thick) layers is sandwiched between an 8000-Å-thick GaAs bottom contact and a 4000-Å-thick GaAs top contact, both of which are doped with Si to a density of  $1 \times 10^{18} \text{ cm}^{-3}$ . An undoped GaAs buffer layer is grown between the substrate and the bottom contact. All samples have the same structural parameters except the two-dimensional (2-D) doping density in the QWs. The GaAs well center is delta-doped with Si to a 2-D density of  $2 \times 10^{11}$ ,  $4 \times 10^{11}$ ,  $6 \times 10^{11}$ , and  $8 \times 10^{11} \text{ cm}^{-2}$  for samples S1, S2, S3, and S4, respectively. The QW parameters (well width and barrier height) chosen here correspond to the optimal condition of having the first excited state in resonance with the barrier height, i.e., the bound-to-quasibound situation.

To facilitate current–voltage, spectral, and responsivity measurements, we fabricated mesa devices with a size of

Manuscript received August 06, 2008; revised September 23, 2008. Current version published April 29, 2009. This work was supported in part by the Natural Science Foundation of China under Contract 60576067.

Y. Yang and W. Z. Shen are with Laboratory of Condensed Matter Spectroscopy and Optoelectronic Physics, Department of Physics, Shanghai Jiao Tong University, Shanghai 200030, China (e-mail: iamyangyao@sjtu.edu.cn; wzshen@sjtu.edu.cn).

H. C. Liu is with the Institute for Microstructural Sciences, National Research Council, Ottawa, ON K1A 0R6, Canada, with the Laboratory of Condensed Matter Spectroscopy and Optoelectronic Physics, Department of Physics, Shanghai Jiao Tong University, Shanghai 200030, China, and also with the National Laboratory for Infrared Physics, Shanghai Institute of Technical Physics, Chinese Academy of Sciences, Shanghai 200083, China (e-mail: h.c.liu@nrc.ca).

N. Li and W. Lu are with National Laboratory for Infrared Physics, Shanghai Institute of Technical Physics, Chinese Academy of Sciences, Shanghai 200083, China (e-mail: ningli@mail.sitp.ac.cn; luwei@mail.sitp.ac.cn).

Z. R. Wasilewski and M. Buchanan are with the Institute for Microstructural Sciences, National Research Council, Ottawa, ON K1A 0R6, Canada (e-mail: zbig.wasilewski@nrc-cnrc.gc.ca; margaret.buchanan@nrc-cnrc.gc.ca).

Color versions of one or more of the figures in this paper are available online at <http://ieeexplore.ieee.org>.

Digital Object Identifier 10.1109/JQE.2009.2013119

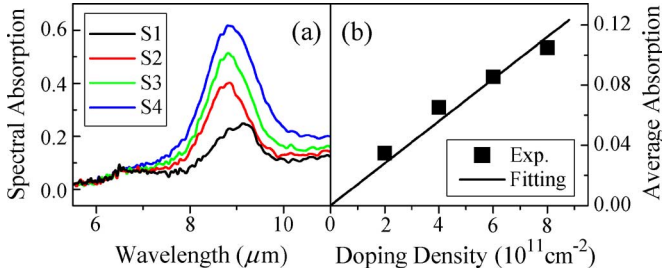


Fig. 1. (a) Spectral absorption at room temperature for 45° incidence and double pass through the multiple QWs. (b) Average absorption efficiency as a function of Si doping density in QWs.

240  $\mu\text{m} \times 240 \mu\text{m}$  using standard photolithographic and wet chemical etching techniques. Both dark and background current-voltage characteristics were tested at temperatures ranging from 50 to 85 K in a closed-cycle refrigerator. Normalized spectral response was measured at 80 K, with the light coupled into the devices from 45° polished facets, and the absolute responsivity was determined with the help of a 500-K calibrated blackbody radiation source. Optical absorption measurements were performed at room temperature.

### III. THEORETICAL BACKGROUND

One of the two most important figures of merit to evaluate infrared photodetector performance is the background-limited infrared performance (BLIP) temperature  $T_{\text{blip}}$ , which is the temperature at which the photocurrent excited by background radiation equals the dark current. Using the standard dark current and responsivity expressions for QWIPs and equating the dark current to the background photocurrent, the relationship between the BLIP temperature and the Fermi energy  $E_f$  is described by the following equation [2]:

$$\eta^{(1)} \tau_{\text{scatt}} \phi_{\text{B,ph}} = \frac{m}{\pi \hbar^2} k_B T_{\text{blip}} \exp\left(\frac{E_f}{k_B T_{\text{blip}}} - \frac{hc}{\lambda_c k_B T_{\text{blip}}}\right) \quad (1)$$

where  $\eta^{(1)}$  is the absorption efficiency for one QW,  $\tau_{\text{scatt}}$  is the scattering time from subband to continuum,  $\phi_{\text{B,ph}}$  is the integrated background photon number flux per unit area incident on the detector,  $m$  is the effective mass of the electron in the wells,  $\hbar$  is the Dirac constant (Planck constant  $h$  divided by  $2\pi$ ),  $k_B$  is the Boltzmann constant,  $c$  is the speed of light, and  $\lambda_c$  is the detector cutoff wavelength. As will be demonstrated later in Fig. 1, the absorption efficiency is proportional to the doping density  $N_D$  and hence the Fermi energy  $E_f$  [ $E_f = (\pi \hbar^2 / m) N_D$ ], and (1) can therefore be rewritten as

$$\frac{E_f}{k_B T_{\text{blip}}} \exp\left(-\frac{E_f}{k_B T_{\text{blip}}}\right) = \text{Constant} \times \exp\left(-\frac{hc}{\lambda_c k_B T_{\text{blip}}}\right). \quad (2)$$

From (2), by maximizing the left-hand side, we can deduce the condition for maximizing BLIP temperature to be  $E_f = k_B T_{\text{blip}}$ .

The other important figure of merit is the detectivity  $D^*(\lambda)$ , which is essentially the signal-to-noise ratio normalized by the

detector area  $A$  and the measurement electrical band width  $\Delta f$ , given by

$$D^*(\lambda) = R(\lambda) \frac{(A \Delta f)^{1/2}}{I_n} \quad (3)$$

where  $I_n$  is the current noise, and the responsivity  $R(\lambda)$  (signal for unit incident power) is expressed as

$$R(\lambda) = \eta(\lambda) \lambda \frac{e}{hc} g \quad (4)$$

where the wavelength-dependent quantum efficiency  $\eta(\lambda)$  equals the absorption efficiency,  $\lambda$  is the wavelength of detected light,  $e$  is the electron charge, and  $g$  is the photoconductive gain.

For QWIPs working at temperatures higher than  $T_{\text{blip}}$ , the current noise is dominated by dark current noise and the corresponding detectivity (detector-noise-limited detectivity)  $D_{\text{det}}^*(\lambda)$  is calculated to be [2]

$$D_{\text{det}}^*(\lambda) = \frac{\eta(\lambda) \lambda}{2hc} \sqrt{\frac{\tau}{N}} \left(\frac{\pi \hbar^2}{mk_B T}\right)^{1/2} \exp\left(\frac{hc}{2\lambda_c k_B T} - \frac{E_f}{2k_B T}\right) \quad (5)$$

where  $\tau$  is the excited carrier lifetime and  $N$  the number of QWs. For the series of studied samples, all parameters are the same except for the absorption and the Fermi energy, both of which depend on the doping density. Since  $\eta(\lambda) \propto E_f$ , we have  $D_{\text{det}}^*(\lambda) \propto E_f \exp(-E_f/2k_B T)$ . We can therefore expect that  $D_{\text{det}}^*(\lambda)$  reaches the maximum value when  $E_f = 2k_B T$ , i.e., the condition for optimized detector-noise-limited detectivity is different from that of the maximized BLIP temperature. It should be noted that the principles of optimization are derived under three assumptions: 1) the increase in Si doping density enhances proportionally the absorption efficiency; 2) the photoconductive gain has a constant value despite the variation of doping density; and 3) the dark current, or equally dark current noise, increases exponentially with the doping density. We will show later that all of these assumptions are valid in our case.

Equations (4) and (5) describe the responsivity and detector-noise-limited detectivity when the device is illuminated by monochrome light with wavelength  $\lambda$ . However, in most practical cases, the detected radiation is broadband covering a range of spectrum. Therefore, it is more appropriate to discuss the detector blackbody responsivity  $R$  and detectivity  $D_{\text{det}}^*$  which involve integration over wavelength

$$R = \frac{\int \eta(\lambda) \lambda \Phi(\lambda) d\lambda}{\int \Phi(\lambda) d\lambda} \frac{e}{hc} g \quad (6)$$

$$D_{\text{det}}^* = \frac{\int \eta(\lambda) \lambda \Phi(\lambda) d\lambda}{\int \Phi(\lambda) d\lambda} \frac{1}{2hc} \sqrt{\frac{\tau}{N}} \left(\frac{\pi \hbar^2}{mk_B T}\right)^{1/2} \cdot \exp\left(\frac{hc}{2\lambda_c k_B T} - \frac{E_f}{2k_B T}\right) \quad (7)$$

where  $\Phi(\lambda)$  is the spectral distribution of incident radiation, which in our study is the illumination from a calibrated 500-K blackbody radiation source. We can further simplify (6) and (7)

by defining a new parameter of the average absorption efficiency  $\bar{\eta}(\Phi)$  of the sample when it is illuminated by the radiation  $\Phi(\lambda)$

$$\bar{\eta}(\Phi) = \frac{\int \eta(\lambda) \lambda \Phi(\lambda) d\lambda}{\lambda_{\text{peak}} \int \Phi(\lambda) d\lambda} \quad (8)$$

where  $\lambda_{\text{peak}}$  is the wavelength corresponding to peak responsivity. Substituting (8) into (6) and (7), we have the following simplified expressions for detector blackbody responsivity and detector-noise-limited detectivity:

$$R = \bar{\eta}(\Phi) \lambda_{\text{peak}} \frac{e}{hc} g \quad (9)$$

$$D_{\text{det}}^* = \frac{\bar{\eta}(\Phi) \lambda_{\text{peak}}}{2hc} \sqrt{\frac{\tau}{N}} \left( \frac{\pi \hbar^2}{mk_{\text{B}}T} \right)^{1/2} \times \exp\left( \frac{hc}{2\lambda_c k_{\text{B}}T} - \frac{E_{\text{f}}}{2k_{\text{B}}T} \right). \quad (10)$$

Equations (9) and (10) indicate that the detector blackbody responsivity  $R$  and detectivity  $D_{\text{det}}^*$  are only different from  $R(\lambda)$  and  $D_{\text{det}}^*(\lambda)$  at a given wavelength  $\lambda$  by a constant factor of  $\bar{\eta}(\Phi) \lambda_{\text{peak}} / \eta(\lambda)$  [i.e., the value of  $D_{\text{det}}^*$  is  $\bar{\eta}(\Phi) / \eta(\lambda_{\text{peak}})$  times the peak detectivity  $D_{\text{det}}^*(\lambda_{\text{peak}})$ ]. As a result,  $D_{\text{det}}^*$  and  $D_{\text{det}}^*(\lambda)$  are expected to have same properties, for example, the optimum condition of  $E_{\text{f}} = 2k_{\text{B}}T$  is also held for  $D_{\text{det}}^*$ .

For photodetectors working at temperatures lower than  $T_{\text{blip}}$ , the detectivity (BLIP detectivity)  $D_{\text{blip}}^*$  is mainly limited by the current noise resulting from the fluctuation of photocurrent induced by background photons. Based on the standard theory [2], once the background photon flux is given,  $D_{\text{blip}}^*$  depends only on the absorption efficiency, or equally the doping density by  $D_{\text{blip}}^* \propto \sqrt{N_{\text{D}}}$ .

#### IV. RESULTS AND DISCUSSION

We start with the investigation of the effect of the doping density on the absorption efficiency, one of the two factors that determine the responsivity. Fig. 1(a) shows the room-temperature absorption spectra of the four QWIP samples. The infrared transmission measurement was done with  $p$ -polarized light incident at the Brewster angle of GaAs. The absorption spectra shown in Fig. 1(a) were converted from the transmission spectra scaled to  $45^\circ$  double-pass equivalent values. It is clear that all samples exhibit near-ideal Lorentzian lineshape absorption characteristics, with approximately the same peak wavelength ( $8.9 \mu\text{m}$ ) and broadening half width ( $1.4 \mu\text{m}$ ). The asymmetry of the absorption spectra is due to the free carrier absorption, which is negligible for short wavelength while obvious for long wavelength region [13]. Employing the measured spectral absorption  $\eta(\lambda)$  and integrating over the wavelength in (8), we get the average absorption efficiency  $\bar{\eta}(\Phi)$  for the four samples under 500-K blackbody radiation [shown as solid squares in Fig. 1(b)]. Since an undoped QWIP would have zero absorption, we fit the data with a straight line through the origin [the solid line in Fig. 1(b)]. This observation demonstrates that the average absorption is proportional to the doping density  $N_{\text{D}}$ , which can be approximated as  $\bar{\eta}(\Phi) = 1.4 \times 10^{-13} \text{ cm}^2 N_{\text{D}}$ . The linear dependence of absorption efficiency on doping

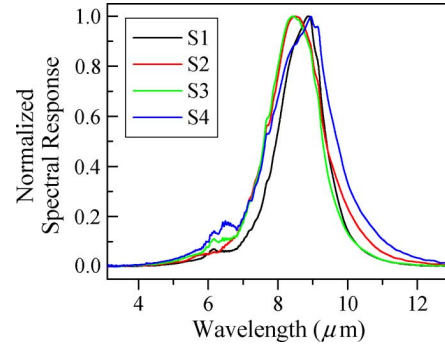


Fig. 2. Normalized spectral response curves measured at 80 K.

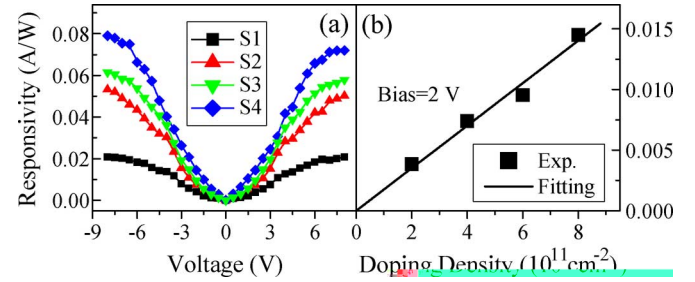


Fig. 3. Absolute responsivity measured at 80 K under 500-K blackbody radiation as a function of (a) bias voltage and (b) Si doping density in QWs.

density is the expected behavior from the simple effective mass theory.

Fig. 2 presents the measured normalized spectral response curves at a device temperature of 80 K. The spectra were taken with a Bomem 100-series Fourier transform spectrometer. For these QWIPs, the spectral becomes quite insensitive to the bias voltage once the voltage is sufficiently large, greater than about 1 V. It is known that the QWIP response spectrum becomes broad at and near zero bias due to the transition to high-lying continuum states in the presence of reduced contribution from the bound-to-quasibound main QWIP response. Once the bias is sufficient so that the escape from the quasi-bound state becomes efficient, the main response dominates and the spectral shape becomes insensitive to bias because of the small Stark shift. The curves shown in Fig. 2 were taken at 10 V. The spectra for the four QWIPs are very similar except a slightly broadening as the doping is increased. All samples have nearly the same cutoff wavelength of  $9.5 \mu\text{m}$ .

Fig. 3(a) illustrates the absolute responsivity  $R$  measured at 80 K as a function of applied bias, when the samples are illuminated by the 500-K blackbody radiation. With bias voltage, this behavior follows the usual QWIP characteristic, i.e., increasing with bias and becoming saturated. Moreover, the responsivity increases with doping. The measured doping-density-dependant responsivity [solid squares in Fig. 3(b)] can be well fitted linearly through the origin [solid line in Fig. 3(b)], confirming that the responsivity is proportional to the doping density. According to (9), the detector blackbody responsivity  $R$  is determined by the product of average absorption efficiency  $\bar{\eta}(\Phi)$  and photoconductive gain  $g$  at a given peak wavelength. Noting that both  $\bar{\eta}(\Phi)$  and  $R$  are proportional to the doping density  $N_{\text{D}}$ , we can therefore deduce that the photoconductive gain  $g$  is independent of

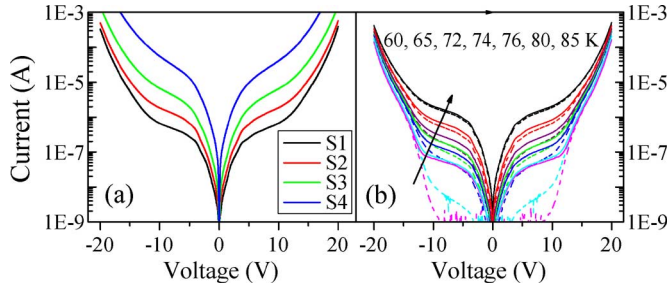


Fig. 4. (a) Dark current properties of the QWIPs under bias voltage between  $-20$  and  $20$  V measured at  $80$  K and (b) Current-voltage characteristics under dark condition and room-temperature background irradiation measured at different temperatures ranged from  $60$  to  $85$  K.

$N_D$ . The variable  $g$  is yielded to be  $0.017$  under  $2$  V bias for the series of studied samples, and increases with the applied bias, resulting in the enhanced responsivity with increasing bias, as shown in Fig. 3(a).

Further understanding of device performance is obtained by dark current investigation, since current noise is mainly resulted from dark current fluctuation for devices operating at detector-noise-limited condition [2]. Fig. 4(a) presents dark current characteristics for the four QWIPs at  $80$  K. Symmetric  $I$ - $V$  characteristic under positive and negative bias is observed, suggesting no significant dopant migration along the growth direction in the samples [14]. The dark current is found to increase exponentially with doping density (e.g., the dark current under  $2$  V bias is  $4.3 \times 10^{-8}$ ,  $8.2 \times 10^{-8}$ ,  $2.0 \times 10^{-7}$ , and  $1.2 \times 10^{-6}$  A for samples S1-S4, respectively). This tendency can be explained by the fact that the dark current of QWIPs is proportional to number of carriers excited above the barrier:  $I_{\text{dark}} \propto \exp[(E_f - E_c)/k_B T]$  [2], where  $E_c$  is the barrier height referenced to the ground state. Since the dark current noise is given by  $I_{n,\text{dark}} = (4egI_{\text{dark}}\Delta f)^{1/2}$  [2], an increase in the doping density also exponentially enhances  $I_{n,\text{dark}}$ .

We now discuss the doping-density-dependent BLIP temperature and detectivity. BLIP temperatures ( $T_{\text{blip}}$ ) were obtained by comparing the measured  $I$ - $V$  curves under dark condition and room-temperature background irradiation at different device temperatures. Fig. 4(b) shows the measured dark (dashed curves) and background  $I$ - $V$  curves (solid curves) of the sample S1 at different temperatures ranging from  $60$  to  $85$  K, from which  $T_{\text{blip}}$  is determined to be  $74$  K. Similarly, the BLIP temperatures of the other samples S2-S4 have been determined to be  $72$ ,  $68$ , and  $64$  K, respectively. Fig. 5(a) displays the theoretical calculation from (2) (solid curve), which is in good agreement with the experimental results (solid squares). According to (2), the condition for the maximized BLIP temperature is predicted to be  $E_f = k_B T_{\text{blip}}$  or equally  $N_D = k_B T_{\text{blip}}(m/\pi\hbar^2)$ . For GaAs-AlGaAs QWIPs with the effective electron mass  $m = 0.067m_e$  in the GaAs wells ( $m_e$  the free electron mass), the calculated doping density that maximizes the BLIP temperature is  $1.8 \times 10^{11} \text{ cm}^{-2}$ , close to sample S1 doping density of  $2 \times 10^{11} \text{ cm}^{-2}$ , whose BLIP temperature is indeed the highest among all samples.

We have further experimentally validated the theoretically predicted condition for optimized detector-noise-limited detec-

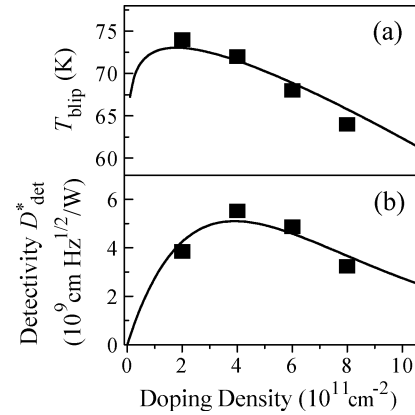


Fig. 5. Dependence of (a) BLIP temperature and (b) detector-noise-limited detectivity measured at  $80$  K under  $500$ -K blackbody radiation on Si doping density in quantum wells.

tivity  $D_{\text{det}}^*$  ( $E_f = 2k_B T$ ). The solid squares in Fig. 5(b) represent the detectivity under  $2$ -V bias measured at  $80$  K. Since the BLIP temperatures of all samples are lower than  $80$  K, all of these QWIPs are working in the detector-noise-limited situation. The solid curve in Fig. 5(b) represents the theoretical results calculated from (10), which fit the measured doping-density-dependent  $D_{\text{det}}^*$ . Sample S2 has the highest measured  $D_{\text{det}}^*$  whose doping density is  $4 \times 10^{11} \text{ cm}^{-2}$ , which is very close to the predicted value of  $3.9 \times 10^{11} \text{ cm}^{-2}$  that maximizes  $D_{\text{det}}^*$ . The excited carrier lifetime used for the fitting is  $11.8$  ps, a reasonable value for GaAs-AlGaAs QWIPs [2]. The underlying physics that the detectivity increases with the doping density until  $2k_B T(m/\pi\hbar^2)$  can be easily understood: doping is needed for QWIPs, since the photon absorption depends linearly on the doping density. However, increasing doping density exponentially enhances the dark current as well as the dark current noise. As a result, the maximized detectivity of QWIPs is only achieved in the doping density that trades off the signal and noise.

The above experimental and theoretical results present a dilemma: we could tune the doping density in the wells to achieve the optimum condition for either the BLIP temperature or the detector-noise-limited detectivity, but could not optimize them both at the same time. Then what condition should be satisfied so that QWIP works at its best performance? Unfortunately, there is no general answer to this question and the choice depends on applications. For example, if for a particular application, providing sufficient cooling is available, one may then want to have the doping on the high side; however, if reaching BLIP at the highest possible temperature is desired, a low value of doping should be used. It is helpful to look at the detectivity as a function of operating temperature  $T$  (shown as the solid curves in Fig. 6). Each curve is divided into two sections by a turning point, the BLIP temperature. The decreasing parts of the curves that correspond to the detector-noise-limited performance are calculated from (10). For QWIPs working at the detector-noise-limited situation, the decrease in temperature would remarkably reduce the current noise and improve the detectivity. However, once the devices have reached the BLIP situation, further reduction in the operating temperature is

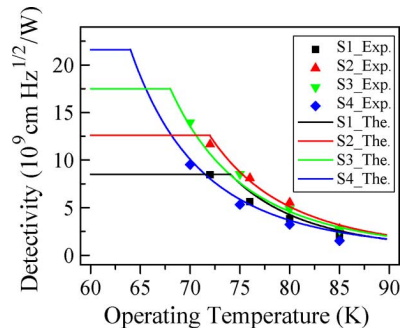


Fig. 6. Detectivity of QWIPs with different doping densities under 500-K blackbody radiation as a function of operating temperature.

useless, since the BLIP detectivity is independent of temperature (the straight lines in Fig. 6). The validity of the theoretical predication is supported by our experimental results, shown as solid symbols in Fig. 6 for the detectivity measured at different temperatures ranged from 70 to 85 K.

Note that some of the curves intercept with each other, and a case-by-case analysis is needed to find the optimum doping density according to the operating temperature. If the desired operating temperature is higher than the maximum BLIP temperature  $T_{\text{blip,max}}$ , QWIPs should be doped to  $2k_{\text{B}}T(m/\pi\hbar^2)$ , since all samples are now working at the detector-noise-limited situation. On the other hand, if  $T$  is below  $T_{\text{blip,max}}$ , the condition for the optimized detector-noise-limited detectivity is no longer the first choice. For QWIPs doped heavier than  $2k_{\text{B}}T_{\text{blip,max}}(m/\pi\hbar^2)$ , the increase in doping density is expected to result in a lower BLIP temperature but a higher BLIP detectivity. As indicated in Fig. 6, the QWIPs should therefore be doped to such a level that the BLIP temperature equals the desired operating temperature. For example, sample S3 has higher detectivity than all other samples at 68 K (the BLIP temperature of sample S3). One may argue that since the QWIP doped to  $k_{\text{B}}T_{\text{blip,max}}(m/\pi\hbar^2)$  (sample S1) has the maximized BLIP temperature, it can be the best choice for some cases. However, Fig. 6 indicates that the detectivity of sample S1 is always lower than sample S2, at all operating temperatures (e.g., although the detectivity of sample S1 has reached its peak value at 74 K, it is still much smaller than that of sample S2, whose BLIP temperature is 72 K). In other words, in comparison with sample S2, the merit of optimized BLIP temperature of sample S1 may not be relevant. All QWIPs whose doping densities are lower than  $2k_{\text{B}}T_{\text{blip,max}}(m/\pi\hbar^2)$  suffer from the same drawback as sample S1 and should be eliminated from our choice list, though they may have high BLIP temperatures.

### V. CONCLUSION

In summary, we have carried out a systematical investigation on the effect of Si doping density in the QWs on properties of QWIPs, including absorption, photoconductive gain, responsivity, dark current, and BLIP temperature and detectivity. The absorption efficiency is revealed to be proportional to doping density, while the photoconductive gain is independent of it. As a result, the responsivity increases with the doping density for

the range of the doping values used here. On the other hand, the detector-noise-limited detectivity is found to increase with doping density for the low doping devices, while it decreases for the high ones, since the dark current, and hence, the dark current noise rise exponentially with  $N_{\text{D}}$ . In addition to the agreement of experimental observation with theoretical results to justify the three assumptions for the principles of optimization, we have confirmed the theoretically predicted conditions for optimized BLIP temperature ( $E_{\text{f}} = k_{\text{B}}T_{\text{blip}}$ ) and detector-noise-limited detectivity ( $E_{\text{f}} = 2k_{\text{B}}T$ ). Based on earlier conclusions, we have furthered the discussion and given the guidelines to reach optimal QWIP performance. We suggest that the optimal doping density of QWIPs should be determined according to the desired operating temperature  $T$ : if  $T$  is higher than the maximized BLIP temperature, QWIPs should be doped to  $2k_{\text{B}}T(m/\pi\hbar^2)$ ; else, QWIPs should be doped to such a level that the BLIP temperature equals the operating temperature.

### REFERENCES

- [1] B. F. Levine, "Quantum-well infrared photodetectors," *J. Appl. Phys.*, vol. 74, no. 8, pp. R1–R81, Oct. 1993.
- [2] H. Schneider and H. C. Liu, *Quantum Well Infrared Photodetectors—Physics and Applications*. Berlin, Germany: Springer-Verlag, 2007, vol. 126, Springer Series in Optical Sciences.
- [3] S. C. Shen, "Comparison and competition between MCT and QW structure material for use in IR detectors," *Microelectron. J.*, vol. 25, no. 8, pp. 713–739, Nov. 1994.
- [4] S. Gunapala, S. V. Bandara, J. K. Liu, J. M. Mumolo, C. J. Hill, S. B. Rafol, D. Zalazar, J. Woolaway, P. D. LeVan, and M. Z. Tidrow, "Towards dualband megapixel QWIP focal plane arrays," *Infrared Phys. Technol.*, vol. 50, no. 2/3, pp. 217–226, Apr. 2007.
- [5] E. Costard and P. Bois, "THALES long wave QWIP thermal imagers," *Infrared Phys. Technol.*, vol. 50, no. 2/3, pp. 260–269, Apr. 2007.
- [6] H. C. Liu, R. Dudek, T. Oogarah, P. D. Grant, Z. R. Wasilewski, H. Schneider, S. Steinkogler, M. Walther, and P. Koidl, "Swept away: QWIPs are fast and can have ideal ( $\sim 100\%$ ) absorption too!," *IEEE Circuits Devices*, vol. 19, no. 6, pp. 9–16, Nov. 2003.
- [7] R. Paiella, F. Capasso, C. Gmachl, D. L. Sivco, J. N. Baillargeon, A. L. Hutchinson, A. Y. Cho, and H. C. Liu, "Self-mode-locking of semiconductor lasers with giant ultrafast optical nonlinearities," *Science*, vol. 290, no. 5497, pp. 1739–1742, Dec. 2000.
- [8] A. G. Steele, H. C. Liu, M. Buchanan, and Z. R. Wasilewski, "Importance of the upper state position in the performance of quantum well intersubband infrared detectors," *Appl. Phys. Lett.*, vol. 59, no. 27, pp. 3625–3627, Dec. 1991.
- [9] A. G. Steele, H. C. Liu, M. Buchanan, and Z. R. Wasilewski, "Influence of the number of wells in the performance of quantum well intersubband infrared detectors," *J. Appl. Phys.*, vol. 72, no. 3, pp. 1062–1064, Aug. 1992.
- [10] H. C. Liu, "Dependence of absorption spectrum and responsivity on the upper state position in quantum well intersubband photodetectors," *J. Appl. Phys.*, vol. 73, no. 6, pp. 3062–3067, Mar. 1993.
- [11] S. K. H. Sim, H. C. Liu, A. Shen, M. Gao, K. F. Lee, M. Buchanan, Y. Ohno, H. Ohno, and E. H. Li, "Effect of barrier width on the performance of quantum well infrared photodetector," *Infrared Phys. Technol.*, vol. 42, no. 3–5, pp. 115–121, Jun. 2001.
- [12] S. D. Gunapala, B. F. Levine, L. Pfeiffer, and K. West, "Dependence of the performance of GaAs/AlGaAs quantum well infrared photodetectors on doping and bias," *J. Appl. Phys.*, vol. 69, no. 9, pp. 6517–6520, May 1991.
- [13] J. S. Blakemore, "Semiconducting and other major properties of gallium arsenide," *J. Appl. Phys.*, vol. 53, no. 10, pp. R123–R181, Oct. 1982.
- [14] H. C. Liu, Z. R. Wasilewski, M. Buchanan, and H. Y. Chu, "Segregation of Si  $\delta$  doping in GaAs–AlGaAs quantum wells and the cause of the asymmetry in the current–voltage characteristics of intersubband infrared detectors," *Appl. Phys. Lett.*, vol. 63, no. 6, pp. 761–763, Aug. 1993.



**Y. Yang** was born in Suizhou, Hubei Province, China, on November 6, 1983. He received the B.S. degree in physics from Shanghai Jiao Tong University, Shanghai, China, in 2006, where he is currently working toward the Ph.D. degree.

His main research interests are related to semiconductor device physics.



**H. C. Liu** (M'99–SM'05–F'07) was born in Taiyuan, China. He received the B.Sc. degree in physics from Lanzhou University, Lanzhou, Gansu, China, in 1982 and the Ph.D. degree in applied physics from the University of Pittsburgh, Pittsburgh, PA, in 1987 as an Andrew Mellon Predoctoral Fellow.

His major research interest is semiconductor quantum devices. He is currently the Imaging Devices Group Leader with the Institute for Microstructural Sciences of the National Research Council of Canada, Ottawa, ON. He is also with

the National Laboratory for Infrared Physics, Shanghai Institute of Technical Physics, Chinese Academy of Sciences, Shanghai, China. He has authored and coauthored approximately 320 refereed journal articles (with about 90 first or sole-authored) and given 110 talks (70 invited) at international conferences, and he holds over a dozen patents.

Dr. Liu is a Fellow of the Academy of Sciences—Royal Society of Canada and a Fellow of the American Physical Society. He was the recipient of the Herzberg Medal from the Canadian Association of Physicists in 2000, the Bessel Prize from the Alexander von Humboldt Foundation in 2001, the Chinese Overseas Distinguished Young Scientist Award (NSFC-B) in 2005, and the overseas Changjiang Chair Professor at Shanghai Jiao Tong University in 2008.



**W. Z. Shen** was born in Suzhou, Jiangsu Province, China, on May 22, 1968. He received the Ph.D. degree in semiconductor physics and semiconductor devices from the Shanghai Institute of Technical Physics, Chinese Academy of Sciences, Shanghai, in 1995.

From 1995 to 1996, he was an Assistant Professor with the National Laboratory for Infrared Physics, Shanghai Institute of Technical Physics. From 1996 to 1999, he was a Research Associate with the Department of Physics and Astronomy, Georgia State

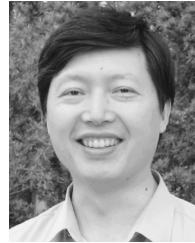
University, Atlanta. Since 1999, he has been with Shanghai Jiao Tong University, Shanghai, where he is currently a full Professor with the Department of Physics and leader of the Condensed Matter Spectroscopy and Optoelectronic Physics Laboratory. His main research interests are in the fields of optical and electrical properties of semiconductors, as well as semiconductor quantum electronic devices and solar cells. He has authored and coauthored more than 100 papers and holds over ten patents.



**N. Li** was born in Shanghai, China, on August 27, 1968. He received the Ph.D. degree in semiconductor physics and semiconductor devices from Shanghai Institute of Technical Physics, Chinese Academy of Sciences, Shanghai, in 1999.

Since 1999, he has been an Assistant Professor, Associate Professor, and Professor with the National Laboratory for Infrared Physics, Shanghai Institute of Technical Physics. His main research interests are in the fields of optical detectors of semiconductors, such as quantum-well infrared photodetectors and

avalanche photodiodes.



**W. Lu** was born in Ningbo, China. He received the B.Sc. degree in physics from Fudan University, China in 1983 and the Ph.D. degree from the National Laboratory for Infrared Physics, Shanghai Institute of Technical Physics, Chinese Academy of Science, Shanghai, in 1988.

His major research interest is optical properties of semiconductors. He is currently the Director of the National Laboratory for Infrared Physics, Shanghai Institute of Technical Physics, Chinese Academy of Sciences. He has authored or coauthored approximately 150 refereed journal articles and holds 40 patents.

Dr. Lu was the recipient of the Alexander von Humboldt Fellowship in 1989.



**Z. R. Wasilewski** received the Ph.D. degree in 1986 from the Institute of Physics, Polish Academy of Sciences, in 1986. His doctoral work focused on the influence of high hydrostatic pressure on the magneto-optical properties of shallow and deep donors in InSb.

He joined the National Research Council of Canada, Ottawa, ON, in 1988, after one year of post-doctoral fellowship with the Imperial College of Science and Technology, London, U.K. Since 1989, his work has been focused primarily on the molecular beam epitaxial growth and characteriza-

tion of III-V semiconductor compounds. He presently holds the position of Principal Research Officer in the Epitaxial and Multilayer Materials of the Institute for Microstructural Sciences at the National Research Council of Canada. He has coauthored over 350 refereed journal articles and conference proceedings.

**M. Buchanan** received the B.Sc. degree in physics in 1965 from the University of Manitoba, Winnipeg, MB, Canada, in 1965 and the Ph.D. degree in solid-state physics from McMaster University, Hamilton, ON, Canada, in 1969.

She joined the National Research Council of Canada, Ottawa, ON, in 1975 and, after working in the Division of Physics and the Division of Energy, joined the Institute for Microstructural Sciences in 1985 as one of a group of three developing the semiconductor device fabrication facilities. She served as Group Leader for the Nanofabrication Group for eight years. She has authored or coauthored more than 290 papers and conference proceedings.